



Article

Systemic Insulin Resistance and Metabolic Perturbations in Chow Fed Inducible Nitric Oxide Synthase Knockout Male Mice: Partial Reversal by Nitrite Supplementation

Hobby Aggarwal ¹, Priya Pathak ¹, Pragati Singh ², Jiaur R. Gayen ², Kumaravelu Jagavelu ¹ and Madhu Dikshit ^{1,3,*}

¹ Pharmacology Division, CSIR-Central Drug Research Institute, Lucknow 226031, India;

hobby.agg@gmail.com (H.A.); priyapathak87@gmail.com (P.P.); kumaraveluj@cdri.res.in (K.J.)

² Pharmaceutics & Pharmacokinetics Division, CSIR-Central Drug Research Institute, Lucknow 226031, India; pragati.bhu@gmail.com (P.S.); jr.gayen@cdri.res.in (J.R.G.)

³ Translational Health Science and Technology Institute, NCR Biotech Science Cluster, 3rd Milestone, Faridabad-Gurgaon Expressway, Faridabad, Haryana 121001, India

* Correspondence: madhudikshit@thsti.res.in or drmadhudikshit@gmail.com; Tel.: +91-129-2876448

Received: 14 June 2020; Accepted: 9 July 2020; Published: 12 August 2020



Abstract: iNOS, an important mediator of inflammation, has emerged as an important metabolic regulator. There are conflicting observations on the incidence of insulin resistance (IR) due to hyperglycemia/dyslipidemia in iNOS^{-/-} mice. There are reports that high fat diet (HFD) fed mice exhibited no change, protection, or enhanced susceptibility to IR. Similar observations were also reported for low fat diet (LFD) fed KO mice. In the present study chow fed iNOS^{-/-} mice were examined for the incidence of IR, and metabolic perturbations, and also for the effect of sodium nitrite supplementation (50 mg/L). In IR-iNOS^{-/-} mice, we observed significantly higher body weight, BMI, adiposity, blood glucose, HOMA-IR, serum/tissue lipids, glucose intolerance, enhanced gluconeogenesis, and disrupted insulin signaling. Expression of genes involved in hepatic and adipose tissue lipid uptake, synthesis, oxidation, and gluconeogenesis was upregulated with concomitant downregulation of genes for hepatic lipid excretion. Nitrite supplementation restored NO levels, significantly improved systemic IR, glucose tolerance, and also reduced lipid accumulation by rescuing hepatic insulin sensitivity, glucose, and lipid homeostasis. Obesity, gluconeogenesis, and adipose tissue insulin signaling were only partially reversed in nitrite supplemented iNOS^{-/-} mice. Our results thus demonstrate that nitrite supplementation to iNOS^{-/-} mice improves insulin sensitivity and metabolic homeostasis, thus further highlighting the metabolic role of iNOS.

Keywords: iNOS^{-/-}; nitrite; nitric oxide; insulin resistance; dyslipidemia; liver; adipose tissue; metabolism

1. Introduction

Nitric oxide (NO), a pleiotropic gaseous signaling molecule, plays an important role in the cardiovascular and metabolic regulations. NO synthesis is catalyzed by Ca²⁺ dependent constitutive NOS (eNOS and nNOS), and Ca²⁺ independent inducible iNOS [1]. Importance of iNOS was primarily studied in infectious diseases, and also in inflammatory conditions [2–5]. Subsequent studies, however, demonstrated constitutive presence of iNOS in various insulin responsive tissues such as liver [6], adipose tissue [7], skeletal muscle [8], and non-responsive tissues/cells like ileum [9], colon [10], and neutrophils [11]. Type 2 diabetes is a complex disease and is exceedingly heterogeneous in its

manifestations with various subtypes necessitating detailed understanding of the mechanisms involved in its pathophysiology for its better management [12]. Insulin resistance (IR) is the key feature of obese diabetics due to altered glucose and lipid homeostasis [13]. Interestingly, genetic polymorphism at the iNOS gene (14-repeat allele) is linked to increased iNOS activity which confers selective advantage to diabetic individuals. This points towards the protective role of constitutive iNOS in preventing or delaying the pathological alterations in diabetes [14,15]. Studies from our group and others on the effect of iNOS derived NO on endothelium functionality have shown that acetylcholine [16] and insulin [17] mediated vasorelaxation was significantly preserved in obese iNOS^{-/-} mice, which was independent of IR, dyslipidemia or hyperglycemia, blood pressure, or oxidative stress. Reduction in NO bioavailability contributes to the pathogenesis of hyperlipidemia, endothelial dysfunction, atherosclerosis, hypertension, diabetes, and obesity [18–20].

Metabolic perturbations and altered insulin sensitivity have been commonly observed in eNOS, nNOS, and triple NOS KO mice [21–23]. Most of the studies on iNOS^{-/-} mice have demonstrated its definitive role in inflammatory [3,5] and infectious conditions [4,24] whereas inconsistent results were reported for its metabolic role [16,25–33]. HFD fed iNOS^{-/-} mice were protected from infiltration of pro-inflammatory macrophages and adipose tissue fibrosis [28]. Likewise, iNOS inhibition reversed hepatic IR and hyperglycemia in obese diabetic mice [34]. These studies suggest that iNOS/NO play an important role in the initiation of IR. Moreover, iNOS^{-/-} mice showed attenuated fructose induced-hepatic steatosis [26], dyslipidemia, IR, and nitrosative stress [27]. Fat deposition in the rat liver and circulatory lipids were, however, increased following iNOS inhibition [35,36]. Likewise, iNOS^{-/-} mice on long term HFD feeding exhibited increased adiposity [25,28,29], and fasting hyperglycemia despite being protected against systemic IR [25]. Our previous studies on LFD or HFD diet fed iNOS^{-/-} mice found them to be IR and also exhibiting perturbed metabolic homeostasis [16,32,37]. Additionally, iNOS^{-/-} mice fed on HFD or LFD displayed significant weight gain, higher fat mass, and dyslipidemia with reduced lean mass [33]. Even chow fed iNOS^{-/-} mice had higher fat mass [30] and circulating triglycerides levels [31]. Above contradictory observations may be due to differing dietary composition, regimens, and also the selection of control groups to interpret the results. In fact, dietary composition (high fat or sugar) can be the important reason of exaggerated inflammation and altered homeostasis.

Studies, both from our group and others, have shown that iNOS^{-/-} mice have decreased NO availability [32,38,39]. Nitrite, a precursor of NO reservoir, is abundant in green leafy vegetables and is also presumably protective against diabetes and cardiovascular diseases [21,40]. As iNOS^{-/-} mice exhibited reductions in the total nitrite content, it is hypothesized that nitrite supplementation in drinking water might compensate for the reduced NO availability. The present study thus investigates the incidence of IR in chow fed iNOS^{-/-} mice, and also the effect of nitrite supplementation on the rescue of systemic, hepatic, and adipose tissue insulin sensitivity. In the present study, the focus was on liver and adipose tissue as they are involved in the regulation of whole-body energy homeostasis and form a highly orchestrated metabolic circuit involving nutrient uptake, processing, transport, and storage. These tissues are shown to be important in the initiation of IR, while association of skeletal muscle has been highlighted in the later stage of disease [41].

2. Research Design and Methods

2.1. Animal Studies

Twelve weeks old, age matched male wild type (WT) and iNOS^{-/-} (Jackson Laboratory, Bar Harbor, ME, USA; 002609) mice on C57BL/6J background were bred and maintained in IVC cages (Tecniplast, Buguggiate, VA, Italy) at 24 ± 2 °C. All procedures were approved by Institutional Animal Ethics Committee of CSIR-CDRI (IAEC/2014/43) in accordance with CPCSEA guidelines. Mice (WT and iNOS^{-/-}) were kept on chow diet (1320, Altromin, Lage, North Rhine-Westphalia, Germany) and glucose tolerance test was performed. WT and iNOS^{-/-} mice then received regular or sodium nitrite (50 mg/L,

NaNO₂) supplemented water ad libitum for 5 weeks as was reported earlier [42,43]. Body weight and length was measured and BMI calculated [44] at the end of 5 weeks of nitrite supplementation.

2.2. Tolerance Tests

Mice fasted for 6 h were administered 2 g/kg D-Glucose, 2 g/kg sodium pyruvate, or 0.6 IU/kg insulin (Human insulin R, Eli Lilly, Indianapolis, IN, USA) by intraperitoneal (i.p.) route for performing glucose (GTT), pyruvate (PTT), or insulin tolerance test (ITT). Blood glucose was monitored using a glucometer (Roche Diagnostics, Mumbai, Maharashtra, India) at 0, 15, 30, 60, and 120 min after administration of glucose, pyruvate, or insulin and area under the curve (AUC) was calculated as described previously [32].

2.3. Body Composition Analysis

Body composition (fat and lean mass) was analyzed by echo MRI (E26-226-RM Echo MRI LLC, Houston, TX, USA) in conscious live mice by applying radio frequency pulses at a distinct static magnetic field [32].

2.4. Indirect Calorimetry

Conscious, unrestrained mice were individually placed in the Oxymax CLAMS (Columbus Instruments, Columbus, OH, USA) with free access to food and water for metabolic measurements [45]. After pre-calibration of system and animal acclimatization, oxygen consumption (VO₂, mL/kg/h), carbon dioxide produced (VCO₂, mL/kg/h) along with food and water intake, RER (VCO₂/VO₂, mL/kg/min), metabolic rates (BMR and RMR) and energy expenditure (kcal/h; heat production) were determined over a 3 day period.

2.5. Serum Biochemistry

Retro-orbital blood was collected from 6 h fasted mice. Estimation of lipids like total cholesterol (TC), triglycerides (TG), low and high density lipoproteins (LDL and HDL), and non-esterified fatty acids (NEFA) were performed in the serum using kits (Randox, Crumlin, Co. Antrim, UK, [16]). Insulin was measured using a kit from Crystal Chem, Elk Grove Village, IL, USA.

2.6. Total Nitrite Estimation

The animals were sacrificed to retrieve the tissues (liver, epididymal white adipose tissues, and hind limb skeletal muscle). Total nitrite (nitrate and nitrite) was estimated in serum (100 µL) and tissues (liver, eWAT, and skeletal muscle, 50 mg) using Griess reagent by reducing nitrate to nitrite using pre-activated cadmium pellets followed by deproteinization in tissue homogenates with 3% trichloroacetic acid [46].

2.7. Tissue Biochemistry

Liver tissue (50 mg) was processed as described previously for the estimation of hepatic total cholesterol [47], triglycerides [48], and free fatty acids [49] using Randox (Crumlin, Co. Antrim, UK) kit.

2.8. Hematoxylin and Eosin (HE) Staining

Formalin fixed and, paraffin embedded adipose tissue (eWAT) was sectioned into 5 µm thin serial slices and HE stained for morphological examination [45]. Adipocytes area was calculated using Adiposoft plugin in Fiji software for Windows 64bit (NIH, Bethesda, MA, USA).

2.9. Oil Red O Staining

Formalin fixed, tissue freezing medium (Leica Biosystems, Ernst-Leitz-Strasse, Wetzlar, Germany) embedded frozen liver tissues were sectioned in 10 µm thin slices, stained with Oil Red O and

counterstained with hematoxylin to visualize the lipid accumulation using Leica QWin version 3.5.1 software [47].

2.10. Western Blot Analysis and Real Time PCR

Insulin was administered at a dose of 0.6 IU/kg i.p. and animals were culled after 30 min to collect organs (liver and eWAT) for Western blot studies along with unstimulated controls in both WT and iNOS^{-/-} mice with or without nitrite supplementation. Liver and adipose tissue protein extracts were subjected to SDS-PAGE, transferred to PVDF membrane, and probed with primary antibodies against Akt or p-Akt^{Ser473} (details listed in Table S1) and visualized with chemiluminescence of horse radish peroxidase-linked secondary anti-rabbit or anti-sheep IgGs using ECL detection solution and normalized with β -actin. Quantitative densitometry was performed using Image J software for Windows 64bit (NIH, Bethesda, MA, USA). Real time PCR was performed as described previously [46] with primers listed in Table S2 and normalized with 18S rRNA.

2.11. Statistical Analysis

Data is presented as mean \pm SEM. Independent unpaired Student's *t* test was used for comparisons as appropriate using GraphPad Prism 7 software. Differences at $p < 0.05$ were considered statistically significant.

2.12. Data Availability

All data supporting the findings of this study are available from the corresponding author on reasonable request.

3. Results

3.1. Gross Parameters, Systemic Insulin, Glucose, Pyruvate Tolerance, and Circulating Lipids

Chow fed iNOS^{-/-} mice at almost similar levels of food consumption weighed more, had higher BMI, body length, and fat mass while lean mass (Figure 1A–E and Figure S1G), VCO₂/heat production, and metabolic rates (BMR and RMR, Figure S1A–C) were less as compared to WT mice. In iNOS^{-/-} mice, total nitrite contents in the serum, liver, adipose tissue, and skeletal muscle were significantly less (Figure 1F,G) along with decreased eNOS expression but with enhanced nNOS in the liver and adipose tissue (Figure S1D–F). Additionally, iNOS^{-/-} mice were glucose intolerant and also had higher circulating glucose levels (Figure 1J) as evident by the persisting increase in circulating glucose levels even 2 h after its administration (Figure 1H,I). iNOS^{-/-} mice also displayed systemic insulin resistance as evident by ITT, PTT (Figure 1M,N,S,T), and increased circulating insulin levels (Figure 1K), HOMA-IR, decreased QUICKI, and unchanged HOMA-B (Figure S1H–J). The relative liver and adipose tissue weights were higher in iNOS^{-/-} mice as compared to WT (Figure 1L). Circulating total cholesterol, triglycerides, NEFA, and LDL were significantly more in iNOS^{-/-} mice while HDL levels were comparable to WT mice (Figure 1O–R and Figure S1K).

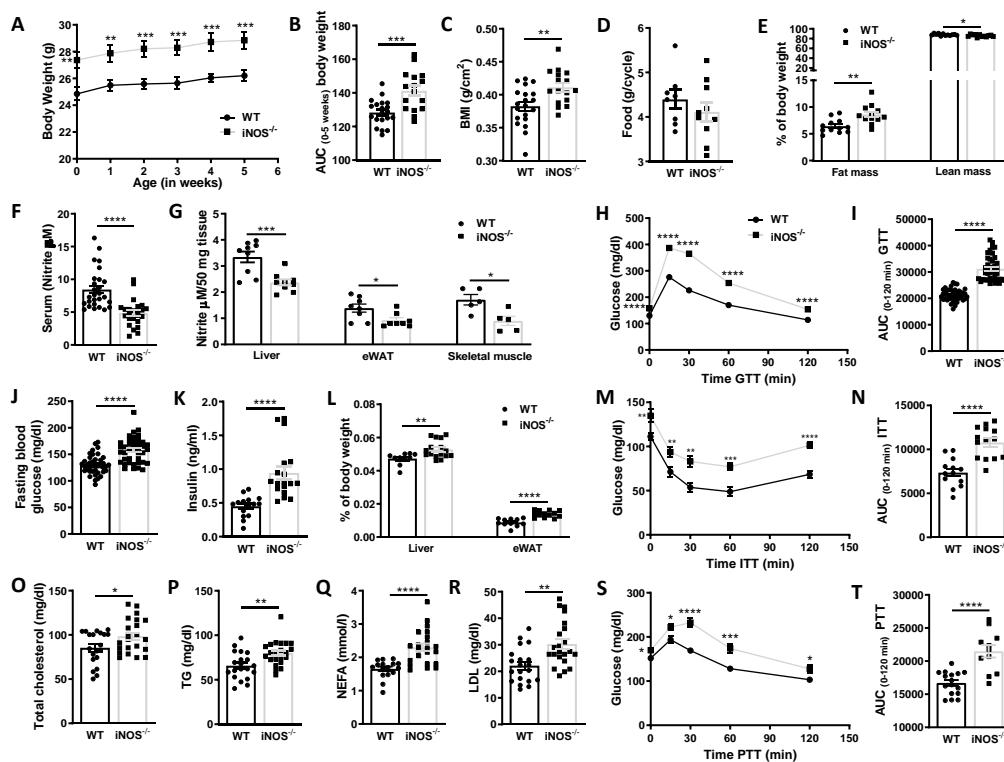


Figure 1. Gross parameters, systemic glucose tolerance, insulin sensitivity, gluconeogenesis, and circulating lipids in chow fed wild type (WT) and *iNOS*^{-/-} mice. (A) Body weight from the initiation (0 week) to study termination (5 weeks) (WT: *n* = 20, *iNOS*^{-/-}: *n* = 16). (B) Area under the curve (AUC) calculated from the gradual change in the body weight of WT and *iNOS*^{-/-} (WT: *n* = 20, *iNOS*^{-/-}: *n* = 16) mice. (C) Body mass index (BMI) (WT: *n* = 20, *iNOS*^{-/-}: *n* = 16), (D) food consumption (WT: *n* = 8, *iNOS*^{-/-}: *n* = 10), (E) whole body fat mass and lean mass (%) (*n* = 12), (F) total nitrite levels in serum (*n* = 24), (G) total nitrite levels in insulin sensitive tissues—liver (*n* = 9), white adipose tissue (*n* = 8), and skeletal muscle (*n* = 5). (H) Intraperitoneal glucose tolerance test (GTT) and (I) area under the curve (AUC) calculated from IPGTT data (*n* = 40). (J) Fasting blood glucose levels (*n* = 40), (K) fasting serum insulin levels (WT: *n* = 16, *iNOS*^{-/-}: *n* = 18), (L) relative liver weight (WT: *n* = 10, *iNOS*^{-/-}: *n* = 16), and epididymal white adipose tissue weight (eWAT) (WT: *n* = 11, *iNOS*^{-/-}: *n* = 12). (M) Intraperitoneal insulin tolerance test (ITT) and (N) AUC calculated from ITT (WT: *n* = 12, *iNOS*^{-/-}: *n* = 10). Serum lipid levels after 6 h fasting (WT: *n* = 16, *iNOS*^{-/-}: *n* = 22). (O) Total cholesterol (TC), (P) triglycerides (TG), (Q) non-esterified free fatty acids (NEFA), (R) low density lipoprotein (LDL). (S) Intraperitoneal pyruvate tolerance test (PTT) and (T) AUC calculated from PTT (WT: *n* = 12, *iNOS*^{-/-}: *n* = 10) in chow fed WT and *iNOS*^{-/-} mice. Data are represented as mean ± SEM. Black circles: WT, black squares: *iNOS*^{-/-} mice. * *p* < 0.05, ** *p* < 0.01, *** *p* < 0.001, **** *p* < 0.0001 vs. WT.

3.2. Status of Metabolic Homeostasis in WT and *iNOS*^{-/-} Mice

3.2.1. Metabolic Homeostasis in the Liver Tissue

iNOS^{-/-} mice had higher lipid accumulation in liver as evident by significant increase in hepatic triglycerides, free fatty acids levels (Figure 2A,B), and Oil red O stained area (Figure 2C). qPCR analysis of transcriptional regulators of lipid synthesis and β -oxidation of fatty acids revealed significantly enhanced expression of PPAR γ and LXR α , and PPAR α , PGC-1 α , and PGC-1 β (Figure 2D). Similarly, the expression of genes involved in the triglyceride synthesis including SREBP-1c, FAS, and ACC1 was also more in KO mice as compared to WT mice (Figure 2E). Expressions of fatty acid uptake genes CD36, SR-1B, and ApoE were significantly enhanced in the liver of *iNOS*^{-/-} mice as compared to WT (Figure 2F). On the other hand, expression of lipid efflux genes, ABCG5 and ABCG8, was however significantly less in the liver of *iNOS*^{-/-} mice (Figure 2G). Moreover, enhanced gluconeogenesis in

iNOS^{-/-} mice correlated with increase in the expression of PC while expression of G6PC, PEPCK, and transcriptional regulator FOXO1 (data not shown) was not altered in the liver (Figure 2H).

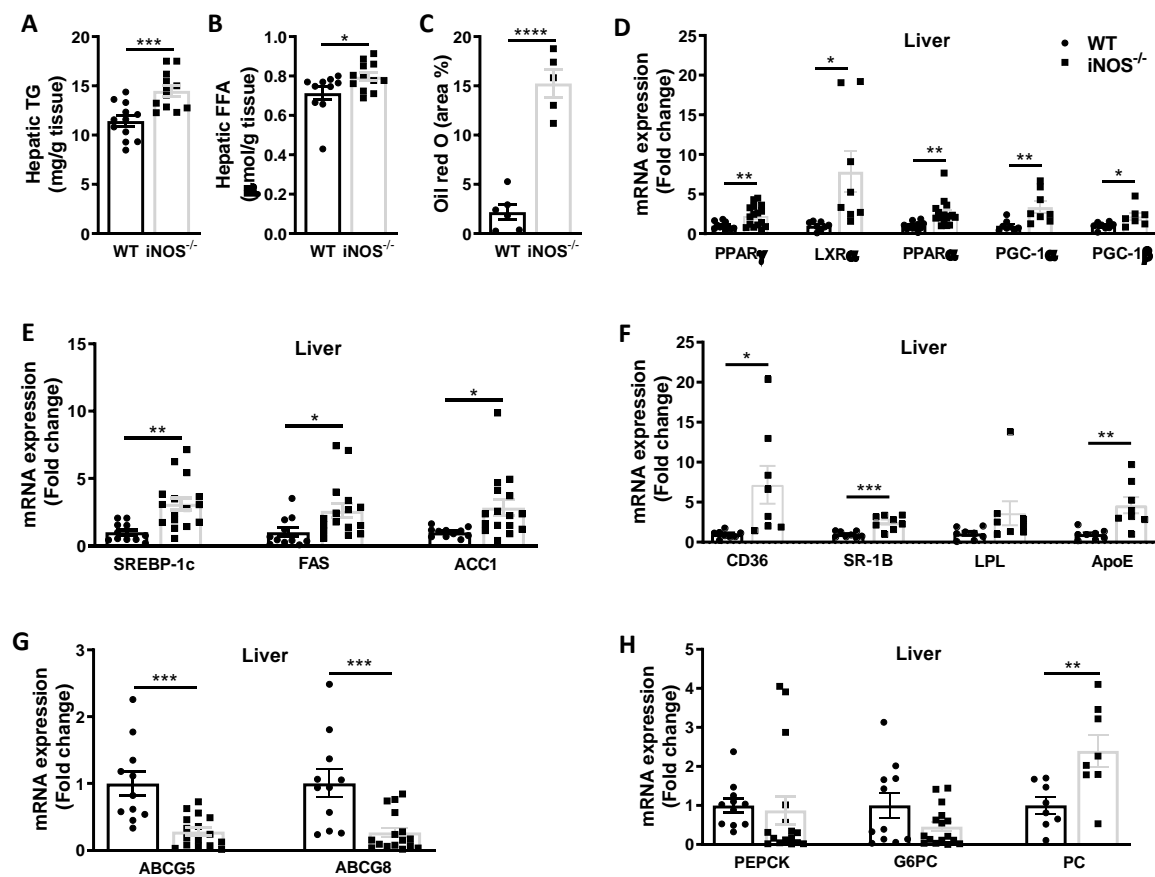


Figure 2. Metabolic homeostasis in liver of chow fed WT and iNOS^{-/-} mice. Lipid accumulation in liver. (A) Hepatic triglycerides ($n = 12$), (B) hepatic free fatty acids (WT: $n = 10$, iNOS^{-/-}, $n = 12$) and (C) hepatic Oil red O staining (WT: $n = 6$, iNOS^{-/-}, $n = 5$). (D) qPCR expressions of transcriptional regulators involved in lipid synthesis: PPAR γ (WT: $n = 11$, iNOS^{-/-}, $n = 16$) and LXR α ($n = 8$) and genes involved in fatty acids oxidation: PPAR α ($n = 11$ – 16), PGC-1 α , and PGC-1 β ($n = 8$). (E) qPCR expression of genes involved in lipid synthesis (WT: $n = 11$, iNOS^{-/-}, $n = 16$): SREBP-1c, FAS, and ACC1. (F) qPCR expression of genes involved in lipid uptake ($n = 8$): CD36, SR-B, ApoE, and LPL. (G) qPCR expression of genes involved in lipid efflux (WT: $n = 11$, iNOS^{-/-}, $n = 16$): ABCG5 and ABCG8. (H) qPCR expression of genes involved in gluconeogenesis (WT: $n = 11$, iNOS^{-/-}, $n = 16$): PEPCK, G6PC, and PC ($n = 8$) in chow fed WT and iNOS^{-/-} mice. Data are represented as mean \pm SEM. Black circles: WT, black squares: iNOS^{-/-} mice. * $p < 0.05$, ** $p < 0.01$, *** $p < 0.001$, **** $p < 0.0001$ vs. WT.

3.2.2. Metabolic Homeostasis in the Adipose Tissue

Enhanced expressions of PPAR γ , LXR α , PPAR α , PGC-1 α , and PGC-1 β in adipose tissue suggest increase in lipogenesis and fatty acids oxidation in iNOS^{-/-} mice in comparison to WT (Figure 3A). Augmentation in the expression of lipogenic genes including SREBP-1c, FAS, and ACC1 was also evident in eWAT of KO mice (Figure 3B). Further, the fatty acid uptake gene-CD36 and lipolysis gene-LPL were also significantly upregulated in the adipose tissue of iNOS^{-/-} mice as compared to WT with increased adipocyte area (Figure 3C,D). Increase in PC (Figure 3E) with no change in the expression of PEPCK and G6PC (Figure 3E) was observed in the adipose tissue of iNOS^{-/-} mice.

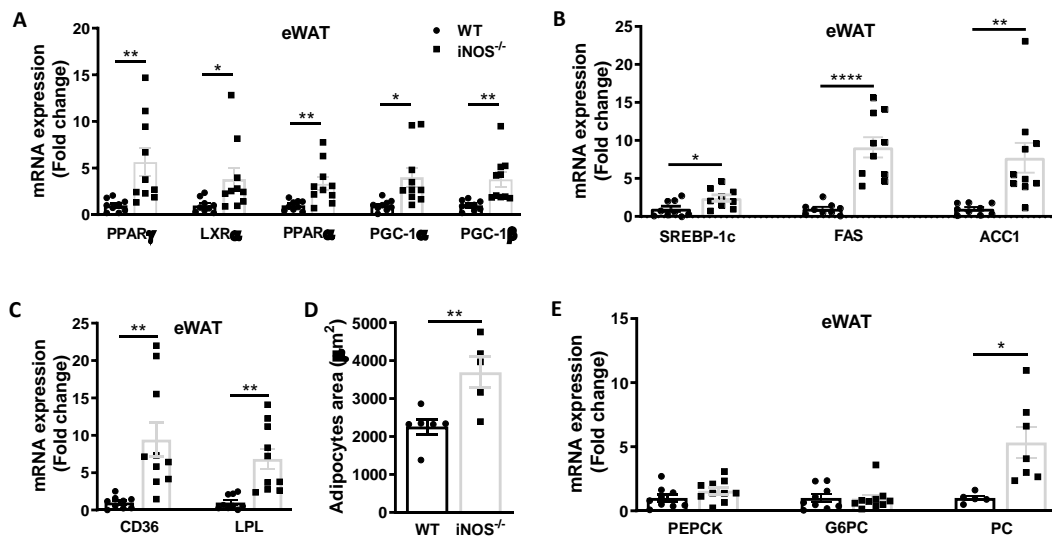


Figure 3. Metabolic homeostasis in adipose tissue of chow fed WT and *iNOS*^{-/-} mice. (A) qPCR expressions of transcriptional regulators involved in lipid synthesis (WT: *n* = 9, *iNOS*^{-/-}: *n* = 10): PPAR γ and LXR α and genes involved in fatty acids oxidation: PPAR α , PGC-1 α , and PGC-1 β . (B) qPCR expression of genes involved in lipid synthesis (WT: *n* = 9, *iNOS*^{-/-}: *n* = 10): SREBP-1c, FAS, and ACC1. (C) qPCR expression of genes involved in lipid uptake (WT: *n* = 9, *iNOS*^{-/-}: *n* = 10): CD36 and LPL. (D) Mean adipocyte area (WT: *n* = 6, *iNOS*^{-/-}: *n* = 5). (E) qPCR expression of genes involved in gluconeogenesis (WT: *n* = 9, *iNOS*^{-/-}: *n* = 10): PEPCK, G6PC, and PC (WT: *n* = 5, *iNOS*^{-/-}: *n* = 7) in chow fed WT and *iNOS*^{-/-} mice. Data are represented as mean \pm SEM. Black circles: WT, black squares: *iNOS*^{-/-} mice. * *p* < 0.05, ** *p* < 0.01, **** *p* < 0.0001 vs. WT.

3.3. Alterations in the Gross Parameters, Glucose Tolerance, Insulin Sensitivity, Gluconeogenesis, and Circulating Lipids after Nitrite Supplementation in Chow Fed *iNOS*^{-/-} Mice

iNOS^{-/-} mice displayed complete reversal in the nitrite content in serum, liver, skeletal muscle, and also adipose tissue upon nitrite supplementation (Figure S2A,B). At similar food/water consumption, and physical activity (data not shown), nitrite supplemented *iNOS*^{-/-} mice exhibited significant reduction in the gross parameters such as BMI, body weight, and fat mass but increased lean mass (Figure S2E–G). VCO₂, heat production, BMR, and RMR along with body length remained unaltered in the nitrite supplemented group (Figure S3A–C,G). Nitrite supplemented *iNOS*^{-/-} animals showed decreased adipose tissue and liver weight (Figure S2J) whereas eNOS mRNA and protein expressions in the liver and adipose tissue were increased (Figure S3D,E) with no change in nNOS (Figure S3F) or iNOS expression (data not shown). Nitrite treatment significantly and partially improved systemic glucose intolerance and blood glucose levels in *iNOS*^{-/-} mice (Figure S2C,D,K). Nitrite supplementation also significantly improved the insulin sensitivity (Figure S2H,I) and restored insulin levels (Figure S2L), HOMA-IR, HOMA-B, and improved QUICKI (Figure S3H–J) in *iNOS*^{-/-} mice. Systemic gluconeogenesis was marginally reduced (*p* < 0.05) after nitrite supplementation in *iNOS*^{-/-} mice (Figure S2M,N). Nitrite supplementation also normalized serum triglycerides and NEFA levels with partial reduction in total cholesterol but had no effect on HDL and LDL levels (Figures S2O–R and 3K). Higher LDL levels in nitrite treated *iNOS*^{-/-} mice correlated with increased LDLR and PCSK9 protein expression in the liver (Figure S2S,T) while LDLR was marginally reduced in *iNOS*^{-/-} mice (Figure S2S). Results of nitrite supplementation in WT mice were as per established literature, and hence are not shown.

3.4. Metabolic Homeostasis in Liver and Adipose Tissue in Chow Fed *iNOS*^{-/-} Mice after Nitrite Supplementation

Expression of genes involved in the lipid synthesis (SREBP-1c, FAS, and ACC1) was reduced in the liver (Figure 4A) and adipose tissue (Figure 5A) of *iNOS*^{-/-} mice following nitrite treatment

and correlates with the reduction in hepatic lipid accumulation (Figure 4F–H) and marginal decrease ($p < 0.05$) in the adipocytes area in eWAT (Figure 5E). However, genes involved in cholesterol synthesis (HMGCoR, SREBP2) were not altered in the liver and adipose of WT, $iNOS^{-/-}$, and nitrite treated $iNOS^{-/-}$ mice (data not shown). Nitrite treatment in $iNOS^{-/-}$ mice reduced G6PC expression (Figure 4B) with no change in PEPCK expression in the liver (Figure 4B) or eWAT (Figure 5B). Similarly, PC expression was marginally but significantly decreased in liver (Figure 4B) and adipose tissue (Figure 5B) in nitrite supplemented $iNOS^{-/-}$ mice.

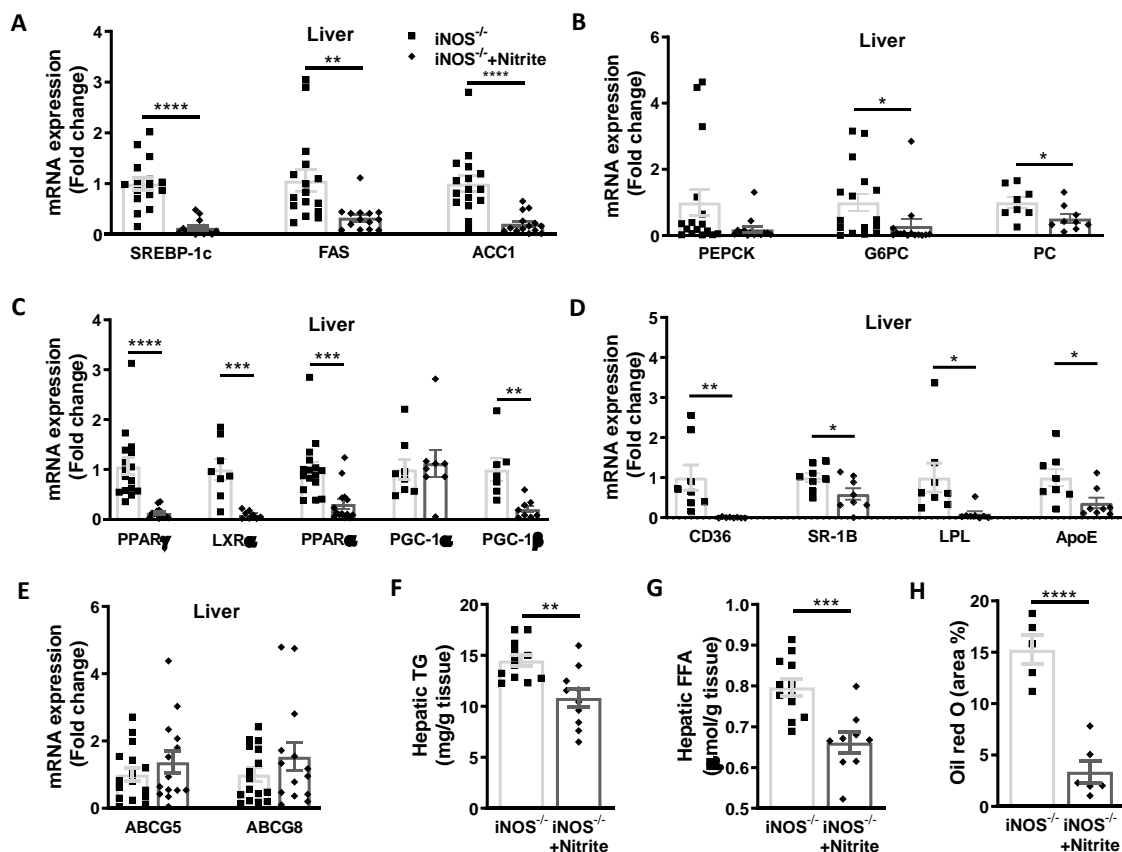


Figure 4. Metabolic homeostasis in liver of chow fed $iNOS^{-/-}$ mice with and without nitrite supplementation. (A) qPCR expression of genes involved in lipid synthesis ($iNOS^{-/-}$: $n = 16$, $iNOS^{-/-}$ + Nitrite: $n = 14$): SREBP-1c, FAS, and ACC1. (B) qPCR expression of genes involved in gluconeogenesis ($iNOS^{-/-}$: $n = 16$, $iNOS^{-/-}$ + Nitrite: $n = 14$): PEPCK, G6PC, and PC ($n = 8$). (C) qPCR expressions of transcriptional regulators involved in lipid synthesis: PPAR γ ($iNOS^{-/-}$: $n = 16$, $iNOS^{-/-}$ + Nitrite: $n = 14$) and LXR α ($n = 8$) and genes involved in fatty acids oxidation: PPAR α ($iNOS^{-/-}$: $n = 16$, $iNOS^{-/-}$ + Nitrite: $n = 14$), PGC-1 α , and PGC-1 β ($n = 8$). (D) qPCR expression of genes involved in lipid uptake ($n = 8$): CD36, SR-B, ApoE, and LPL. (E) qPCR expression of genes involved in lipid efflux ($iNOS^{-/-}$: $n = 16$, $iNOS^{-/-}$ + Nitrite: $n = 14$): ABCG5 and ABCG8. Lipid accumulation in liver, (F) hepatic triglycerides ($iNOS^{-/-}$: $n = 12$, $iNOS^{-/-}$ + Nitrite: $n = 10$), (G) hepatic free fatty acids ($iNOS^{-/-}$: $n = 12$, $iNOS^{-/-}$ + Nitrite: $n = 10$), and (H) hepatic Oil red O staining ($iNOS^{-/-}$: $n = 5$, $iNOS^{-/-}$ + Nitrite: $n = 6$) in chow fed $iNOS^{-/-}$ mice with or without nitrite supplementation. Data are represented as mean \pm SEM. Black squares: $iNOS^{-/-}$ mice without nitrite supplementation, black diamonds: $iNOS^{-/-}$ mice with nitrite supplementation. * $p < 0.05$, ** $p < 0.01$, *** $p < 0.001$, **** $p < 0.0001$ vs. $iNOS^{-/-}$.

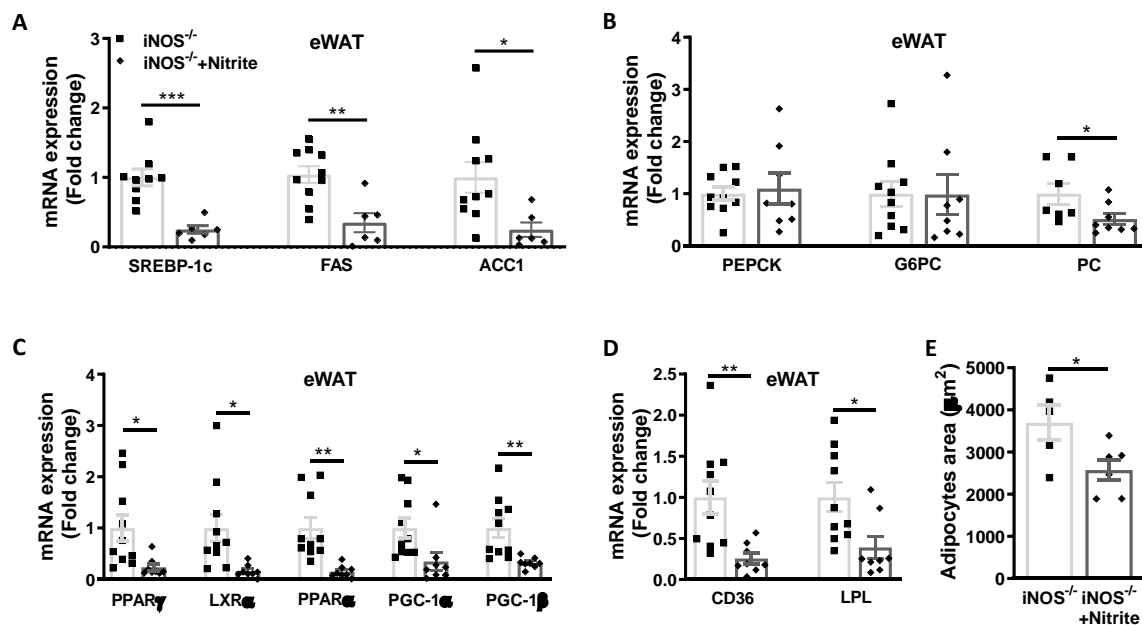


Figure 5. Metabolic homeostasis in adipose tissue of chow fed WT and $iNOS^{-/-}$ mice with and without nitrite supplementation. (A) qPCR expression of genes involved in lipid synthesis ($iNOS^{-/-}$: $n = 10$, $iNOS^{-/-}$ + Nitrite: $n = 6$): SREBP-1c, FAS, and ACC1. (B) qPCR expression of genes involved in gluconeogenesis ($iNOS^{-/-}$: $n = 10$, $iNOS^{-/-}$ + Nitrite: $n = 8$): PEPCK, G6PC, and PC ($iNOS^{-/-}$: $n = 7$, $iNOS^{-/-}$ + Nitrite: $n = 8$). (C) qPCR expressions of transcriptional regulators involved in lipid synthesis ($iNOS^{-/-}$: $n = 10$, $iNOS^{-/-}$ + Nitrite: $n = 8$): PPAR γ and LXR α and genes involved in fatty acids oxidation: PPAR α , PGC-1 α , and PGC-1 β . (D) qPCR expression of genes involved in lipid uptake ($iNOS^{-/-}$: $n = 10$, $iNOS^{-/-}$ + Nitrite: $n = 8$): CD36 and LPL. (E) Mean adipocyte area ($iNOS^{-/-}$: $n = 5$, $iNOS^{-/-}$ + Nitrite: $n = 6$) in chow fed $iNOS^{-/-}$ mice with or without nitrite supplementation. Data are represented as mean \pm SEM. Black squares: $iNOS^{-/-}$ mice without nitrite supplementation, black diamonds: $iNOS^{-/-}$ mice with nitrite supplementation. * $p < 0.05$, ** $p < 0.01$, *** $p < 0.001$ vs. $iNOS^{-/-}$.

Expression of PPAR γ and LXR α was normalized after nitrite supplementation in liver (Figure 4C) and adipose tissue (Figure 5C). PPAR α and PGC-1 β expression in liver (Figure 4C) and adipose tissue (Figure 5C) was significantly reduced following nitrite supplementation to $iNOS^{-/-}$ mice. PGC-1 α was decreased in adipose tissue of nitrite treated $iNOS^{-/-}$ mice (Figure 5C) but not in liver (Figure 4C). Expression of CD36, SR-1B, ApoE, and lipolysis gene, LPL in liver (Figure 4D), and CD36 and LPL in adipose tissue (Figure 5D) was regressed by nitrite supplementation in $iNOS^{-/-}$ mice. ABCG5 and ABCG8 expression remained unaltered after nitrite supplementation in $iNOS^{-/-}$ mice (Figure 4E).

3.5. Insulin Signaling in Nitrite Supplemented Chow Fed WT and $iNOS^{-/-}$ Mice

Metabolic homeostasis is primarily regulated by insulin signaling via Akt in the insulin sensitive organs. Total Akt expression was reduced significantly in the liver and adipose tissue of $iNOS^{-/-}$ mice as compared to WT, and after nitrite treatment was restored in the liver (Figure 6A) but only marginally in the adipose tissue in $iNOS^{-/-}$ mice (Figure 6C). Akt-1/2/3 phosphorylation (Ser473) was also significantly reduced in the liver of $iNOS^{-/-}$ mice as compared to WT, which was completely reversed after nitrite supplementation (Figure 6B). Nitrite significantly enhanced the p-Akt levels in the adipose tissue of WT mice but not in the $iNOS^{-/-}$ mice (Figure 6D).

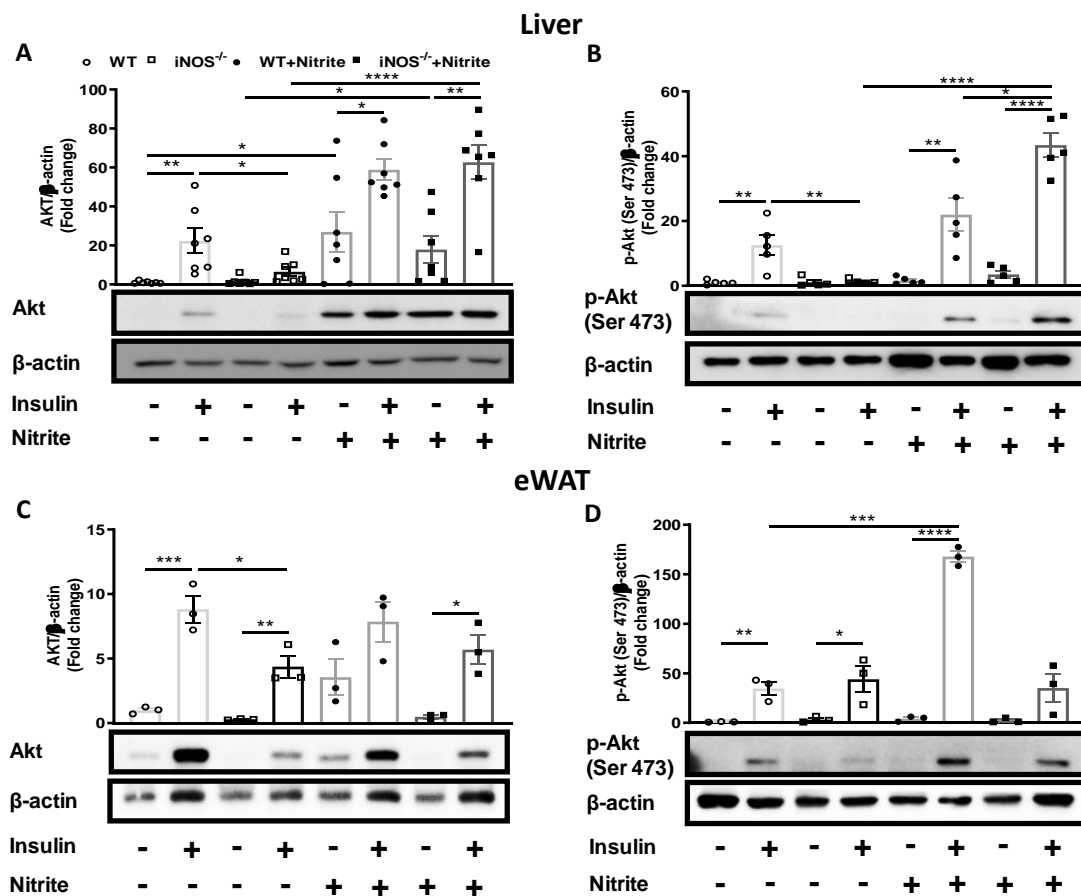


Figure 6. Insulin signaling in chow fed WT and iNOS^{-/-} mice and its alteration by nitrite treatment. Immunoblots of liver (A) Akt-1/2/3 ($n = 7$) and (B) p-Akt-1/2/3 ($n = 5$). Immunoblots of adipose tissue ($n = 3$) (C) Akt-1/2/3 and (D) p-Akt-1/2/3. Bar diagrams represent mean \pm SEM in chow fed, control, or nitrite treated WT and iNOS^{-/-} mice in both basal and insulin stimulated conditions. White circles: WT; black circles: WT supplemented with nitrite; white squares: iNOS^{-/-}; black squares: iNOS^{-/-} supplemented with nitrite. * $p < 0.05$, ** $p < 0.01$, *** $p < 0.001$, **** $p < 0.0001$ between indicated groups.

4. Discussion

Single (eNOS) [21], double (eNOS/nNOS) [22], and triple (eNOS, nNOS, and iNOS) [23] NOS knockout mice are IR and display metabolic perturbations. Studies conducted so far on iNOS^{-/-} mice used several dietary fats such as lard or vegetable oils [25,29,32,33,50] among which lard is more obesogenic and diabetogenic [51]. In addition, dietary regimens and protocols to examine the role of iNOS in IR, obesity, and diabetes [25,27,29,33,50] were also different reporting either IR and dyslipidemia [16,31–33] or protection against IR as outcome [25–30]. The decreased NO bioavailability in endothelial dysfunction, atherosclerosis, diabetes, obesity, and metabolic syndrome is well established. The role of iNOS as a pro-inflammatory agent is also well established but its protective role under normal physiological conditions, and cardiovascular disorders is less investigated. The present comparative study was therefore undertaken in chow fed iNOS KO, and WT mice to systematically assess insulin sensitivity by monitoring systemic (GTT, ITT, PTT), tissue (insulin signaling), biochemical (glucose and lipids), and molecular (lipid and glucose metabolism) parameters, as well as by calorimetry using a comprehensive lab animal monitoring system. Furthermore, metabolic perturbations were evaluated at the hepatic and adipose tissue level by investigating expressions of crucial genes and insulin signaling.

iNOS^{-/-} mice fed on chow diet [30], LFD [32,33], or HFD [25,28,33] exhibited gain in weight and fat mass with no change in food intake [28]. We also observed that weight gain by iNOS^{-/-} mice with

similar food intake, correlated both with increase in body fat and decrease in lean mass. In addition, *iNOS*^{-/-} mice in the present study displayed so far unreported higher BMI and body length (Figure 1C and Figure S1G). On the contrary no change in the body weight in KO mice was reported [27,29,39,50] even with higher chow or HFD intake [25,29]. These observed discrepancies can be ascribed to the differences in the protocols and diets used in the studies [25,27–30,39].

Non-specific NOS inhibition enhanced serum and hepatic lipids in rodents [35,36] and increased eWAT and perirenal fat deposits [52]. Area of adipocytes was also enhanced in *iNOS*^{-/-} mice fed on chow diet or HFD diet for 16–18 weeks [25,28,29] suggesting a link between absence of *iNOS* and increased adiposity. In the present study we observed significant reduction in VCO₂, heat production, and metabolic rates with no change in the physical activity in chow fed *iNOS*^{-/-} mice. Low BMR and RMR are associated with metabolic thrift, weight gain, and obesity [53]. Interestingly Nakata et al. reported increase in triglycerides in chow fed *iNOS*^{-/-}, *nNOS*^{-/-}, *eNOS*^{-/-}, *n/i/eNOS*^{-/-} mice [31]. Kakimoto et al. also found increased lipids in *iNOS*^{-/-} mice 4 weeks after LFD or HFD feeding [33] even though they used C57BL/6N mice which are less prone to obesity due to intact NNT activity. Moreover, Nozaki et al. showed increased circulating and hepatic NEFA in HFD fed *iNOS*^{-/-} mice while others did not find change in the lipids [26,27,29,30]. Our findings thus confirm the obese phenotype of *iNOS*^{-/-} mice.

Blood glucose, AUC values of GTT and IIT, as shown in a recently published report [54], were similar to our findings in KO mice. Perreault et al. also showed systemic hyperglycemia [25], and Cha et al. found marginally increased insulin levels [30,39]. Incidentally, in some of the reports, basal glucose levels in WT mice were on the higher side [28,55]. GTT was mostly conducted using 1 g/kg dose of glucose [25,28,29,31,33] while in the present study we used 2 g/kg glucose in a relatively large number (>30) of *iNOS*^{-/-} mice. Moreover, our finding on PTT support the enhanced gluconeogenesis in KO mice.

Expectedly, total nitrite levels in *iNOS*^{-/-} mice were significantly less as has also been reported by others [27,28,32,38,39,50] with decreased *eNOS* and increased *nNOS* expression in liver and adipose tissue. This might be due to compensatory mechanisms developed due to the loss of a particular NOS gene. Interestingly, low nitrite diet fed mice displayed glucose intolerance, IR, and high circulating lipid levels [19]. Nitrite acts a precursor for NO generation in saliva, stomach, blood, urine, and skin through enzymatic and non-enzymatic mechanisms and it was thus hypothesized that it may compensate the reduced NO availability in the *iNOS*^{-/-} mice. Nitrite supplementation to *iNOS*^{-/-} mice reversed insulin sensitivity, insulin levels, augmented lean mass, decreased fat mass and liver weight, with partial yet significant rescue in glucose levels, glucose tolerance, and gluconeogenesis. These findings suggest nutrition based strategies, like use of green leafy vegetables and other nitrite rich foods, against IR. Nitrate/nitrite treatment also improved glucose intolerance in *eNOS*^{-/-} mice [21,56], reduced fasting blood glucose in db/db mice [42], rescued glucose intolerance and HOMA-IR in diabetic KKA^y mice [43], and reversed insulin levels with improvement in GTT and PTT in HFD fed diabetic rats [57]. Reduction in RMR and VO₂ with no change in RER has also been reported in healthy human volunteers after nitrate supplemented diet [58]. Moreover, long term treatment with nitrate/nitrite also improved blood glucose, insulin sensitivity with decreased insulin and HOMA-IR in WT mice [59] as also observed by us. Likewise, no significant change in LDL levels was observed upon nitrite treatment [19,57]. This can be due to increased PCSK9 expression in liver along with enhanced expression of LDLR. The marginal effect of nitrite on obesity related parameters [19,43,56,57] cannot be explained only on the basis of reversal in NO levels and *eNOS* expression in KO mice [19]. Partial reversal of adiposity by nitrite supplementation in *iNOS*^{-/-} mice suggests a role of other regulators in metabolic perturbations. Moreover, recent advances have made us more aware of gut microbiota contribution to metabolic disorders through an axis of communication with adipose tissue regulating body weight and metabolism [60]. However, the role of gut microbiome has not been examined so far in the *iNOS*^{-/-} mice thus warranting further investigations on these lines.

Gene expression analysis data correlates with the functional and biochemical findings in *iNOS*^{-/-} mice. Unaltered expression of G6PC and PEPCK in *iNOS*^{-/-} mice were observed earlier [27], and PPAR γ expression was also reported to be increased in eWAT of HFD fed *iNOS*^{-/-} mice [29]. Increase in the expression of SREBP-1c and LPL in the adipose tissue also correlated with profound increase in the circulating NEFA as was observed during *iNOS* inhibition induced lipolysis in the adipose tissue [61]. PGC-1 α induction promotes mitochondrial biogenesis as well as augmented gluconeogenic gene expression and increased lipid oxidation in altered metabolic states [62]. Increased PGC-1 α in eWAT of HFD fed *iNOS*^{-/-} mice was also observed earlier [28]. Lipolysis in the adipose tissue promotes supply of fatty acids and acetyl CoA to the liver to enhance glucose production via PC activation [63]. Induction in PC expression (Figure 2H) supports enhanced gluconeogenesis, which was previously not examined in *iNOS*^{-/-} mice. Nitrite treatment marginally reversed the induction in PC expression but not that of PGC-1 α in the liver (Figure 4C). Increase in PPAR γ expression in the liver and adipose tissue of *iNOS*^{-/-} mice was normalized by the nitrite treatment. The present study extensively examined IR and insulin signaling in the liver of *iNOS*^{-/-} mice and found disrupted insulin signaling unlike earlier studies which show no change [25,27,29]. Interestingly, *iNOS*^{-/-} mice fed on chow diet showed significant increase in fat mass and marginal reduction in the insulin signaling (PI3K-Akt axis) [30]. Reduction in the sensitivity of insulin signaling in liver and adipose tissue of *iNOS*^{-/-} mice was rescued by nitrite treatment in liver but not in adipose tissue providing an explanation for the partial recovery of obese phenotype in *iNOS*^{-/-} mice. The present study, by using a multipronged approach, thus highlights the importance of *iNOS* in maintaining glucose and lipid homeostasis, and IR.

5. Conclusions

The present study was aimed at characterizing adult *iNOS*^{-/-} mice for IR by systematically evaluating the phenotypic, biochemical, functional parameters and also by limited analysis of important genes. Chow fed adult *iNOS*^{-/-} mice like other *NOS*^{-/-} mice exhibited systemic IR, dyslipidemia, and metabolic perturbations. Improvement in IR after nitrite supplementation correlated with compensated NO levels which partially reversed the gluconeogenesis, dysregulated insulin signaling, and weight gain suggesting the beneficial role of homeostatic *iNOS*/NO in metabolic regulation. The results obtained thus demonstrate the important contribution of liver and adipose tissue in impacting the insulin sensitivity in *iNOS*^{-/-} mice.

Supplementary Materials: The following are available online at <http://www.mdpi.com/2076-3921/9/8/736/s1>. Figure S1: Systemic metabolic homeostasis and NOS isoforms expression in chow fed WT and *iNOS*^{-/-} mice. Figure S2: Gross parameters, systemic glucose tolerance, insulin sensitivity, gluconeogenesis and lipids in chow fed *iNOS*^{-/-} mice with or without nitrite supplementation. Figure S3: Systemic metabolic homeostasis and NOS isoforms expression in chow fed *iNOS*^{-/-} mice with and without nitrite supplementation. Table S1: List of primary antibodies used and their working dilutions. Table S2: Primers list for qPCR in mice.

Author Contributions: H.A. performed most of the experiments and wrote the first draft of the manuscript. P.P. performed some experiments. P.S. performed OxyCLAMS experiments. J.R.G. provided critical inputs and interpretation for oxyCLAMS studies/data. K.J. provided the animals and critical suggestions during the study. M.D. conceptualized the whole project, designed, supervised the studies, and interpreted the data as presented in the article; she also finalized the manuscript. M.D. is the guarantor of this work and, as such, had full access to all the data in the study and takes responsibility for the integrity of the data and accuracy of the data analysis. All authors have read and agreed to the published version of the manuscript.

Funding: The present study was supported by JC Bose National fellowship [SB/SE/JCB-017/2015] to Madhu Dikshit. Research fellowships to HA from Indian Council of Medical Research, PP from Council of Scientific and Industrial Research and PS from University Grants Commission, India are acknowledged. This manuscript has CSIR-CDRI communication no. 10093.

Conflicts of Interest: The authors declare no conflict of interest. The funders had no role in the design of the study; in the collection, analyses, or interpretation of data; in the writing of the manuscript, or in the decision to publish the results.

Abbreviations

ABCG5/8	ATP-binding cassette subfamily G member 5/8;
ACC1	Acetyl-CoA carboxylase 1;
ApoE	Apolipoprotein E;
BMI	Body mass index;
BMR	Basal metabolic rate;
CD36	Cluster of differentiation 36;
eNOS	Endothelial-nitric oxide synthase;
eWAT	epididymal white adipose tissue;
FAS	Fatty acid synthase;
FoxO1	Forkhead box O1
G6PC	Glucose-6-phosphatase;
HFD	High fat diet;
HMGCoR	3-hydroxy-3-methyl-glutaryl-coenzyme A reductase;
HOMA-IR	Homeostatic Model Assessment of Insulin Resistance;
iNOS ^{-/-}	Inducible-nitric oxide synthase knockout;
IPGTT	Intra-peritoneal glucose tolerance test;
IR	Insulin resistance;
ITT	Insulin tolerance test;
KO	Knock out
LDLR	Low-Density Lipoprotein Receptor;
LFD	Low fat diet;
LPL	Lipoprotein Lipase;
LXR	Liver X receptor;
nNOS	Neuronal-nitric oxide synthase;
NO	Nitric oxide;
pAkt	phospho protein kinase B;
PC	Pyruvate carboxylase;
PCSK9	Proprotein convertase subtilisin/kexin type 9;
PEPCK	Phosphoenolpyruvate carboxykinase;
PGC	Peroxisome proliferator-activated receptor- γ coactivator;
PI3K	Phosphoinositide 3-kinases;
PPAR	Peroxisome proliferator-activated receptor;
PTT	Pyruvate tolerance test;
QUICKI	Quantitative insulin-sensitivity check index;
RER	Respiratory Exchange Ratio;
RMR	Resting metabolic rate;
SR-1B	Scavenger receptor, class B type 1;
SREBP-1c	Sterol regulatory element-binding protein 1c;
VLDL	Very-low-density lipoprotein;
WT	Wild type

References

1. Anavi, S.; Tirosh, O. iNOS as a metabolic enzyme under stress conditions. *Free Radic. Biol. Med.* **2020**, *146*, 16–35. [[CrossRef](#)] [[PubMed](#)]
2. Villanueva, C.; Giulivi, C. Subcellular and cellular locations of nitric oxide synthase isoforms as determinants of health and disease. *Free Radic. Biol. Med.* **2010**, *49*, 307–316. [[CrossRef](#)] [[PubMed](#)]
3. Wong, J.M.; Billiar, T.R. Regulation and Function of Inducible Nitric Oxide Synthase during Sepsis and Acute Inflammation. *Adv. Pharmacol.* **1995**, *34*, 155–170. [[CrossRef](#)] [[PubMed](#)]
4. Kröncke, K.D.; Fehsel, K.; Kolb-Bachofen, V. Inducible nitric oxide synthase in human diseases. *Clin. Exp. Immunol.* **1998**, *113*, 147–156. [[CrossRef](#)]

5. House, L.M.; Morris, R.T.; Barnes, T.M.; Lantier, L.; Cyphert, T.J.; McGuinness, O.P.; Otero, Y.F. Tissue inflammation and nitric oxide-mediated alterations in cardiovascular function are major determinants of endotoxin-induced insulin resistance. *Cardiovasc. Diabetol.* **2015**, *14*, 56. [[CrossRef](#)]
6. McNaughton, L.; Puttagunta, L.; Martinez-Cuesta, M.A.; Kneteman, N.; Mayers, I.; Moqbel, R.; Hamid, Q.; Radomski, M.W. Distribution of nitric oxide synthase in normal and cirrhotic human liver. *Proc. Natl. Acad. Sci. USA* **2002**, *99*, 17161–17166. [[CrossRef](#)] [[PubMed](#)]
7. Elizalde, M.; Rydén, M.; van Harmelen, V.; Eneroth, P.; Gyllenhammar, H.; Holm, C.; Ramel, S.; Olund, A.; Arner, P.; Andersson, K. Expression of nitric oxide synthases in subcutaneous adipose tissue of nonobese and obese humans. *J. Lipid Res.* **2000**, *41*, 1244–1251.
8. Park, C.-S.; Park, R.; Krishna, G. Constitutive expression and structural diversity of inducible isoform of nitric oxide synthase in human tissues. *Life Sci.* **1996**, *59*, 219–225. [[CrossRef](#)]
9. Hoffman, R.A.; Zhang, G.; Nussler, N.C.; Gleixner, S.L.; Ford, H.R.; Simmons, R.L.; Watkins, S.C. Constitutive expression of inducible nitric oxide synthase in the mouse ileal mucosa. *Am. J. Physiol. Liver Physiol.* **1997**, *272*, G383–G392. [[CrossRef](#)]
10. Perner, A.; Andresen, L.; Normark, M.; Rask-Madsen, J. Constitutive Expression of Inducible Nitric Oxide Synthase in the Normal Human Colonic Epithelium. *Scand. J. Gastroenterol.* **2002**, *37*, 944–948. [[CrossRef](#)]
11. Saini, R.; Patel, S.; Saluja, R.; Sahasrabudhe, A.A.; Singh, M.P.; Habib, S.; Bajpai, V.K.; Dikshit, M. Nitric oxide synthase localization in the rat neutrophils: Immunocytochemical, molecular, and biochemical studies. *J. Leukoc. Biol.* **2006**, *79*, 519–528. [[CrossRef](#)] [[PubMed](#)]
12. Ahlqvist, E.; Storm, P.; Käräjämäki, A.; Martinell, M.; Dorkhan, M.; Carlsson, A.; Vikman, P.; Prasad, R.B.; Aly, D.M.; Almgren, P.; et al. Novel subgroups of adult-onset diabetes and their association with outcomes: A data-driven cluster analysis of six variables. *Lancet Diabetes Endocrinol.* **2018**, *6*, 361–369. [[CrossRef](#)]
13. Ormazabal, V.; Nair, S.; Elfeky, O.; Aguayo, C.; Salomon, C.; Zuñiga, F.A. Association between insulin resistance and the development of cardiovascular disease. *Cardiovasc. Diabetol.* **2018**, *17*, 122. [[CrossRef](#)] [[PubMed](#)]
14. Warpeha, K.M.; Xu, W.; Liu, L.; Charles, I.G.; Patterson, C.C.; Ah-Fat, F.; Harding, S.; Hart, P.M.; Chakravarthy, U.; Hughes, A.E. Genotyping and functional analysis of a polymorphic (CCTT) (n) repeat of NOS2A in diabetic retinopathy. *FASEB J.* **1999**, *13*, 1825–1832. [[CrossRef](#)] [[PubMed](#)]
15. Johannesen, J.; Tarnow, L.; Parving, H.H.; Nerup, J.; Pociot, F. CCTT-repeat polymorphism in the human NOS2-promoter confers low risk of diabetic nephropathy in type 1 diabetic patients. *Diabetes Care* **2000**, *23*, 560–562. [[CrossRef](#)]
16. Pathak, P.; Kanshana, J.S.; Kanuri, B.; Rebello, S.C.; Aggarwal, H.; Jagavelu, K.; Dikshit, M. Vasoreactivity of isolated aortic rings from dyslipidemic and insulin resistant inducible nitric oxide synthase knockout mice. *Eur. J. Pharmacol.* **2019**, *855*, 90–97. [[CrossRef](#)]
17. Noronha, B.T.; Li, J.-M.; Wheatcroft, S.B.; Shah, A.M.; Kearney, M.T. Inducible nitric oxide synthase has divergent effects on vascular and metabolic function in obesity. *Diabetes* **2005**, *54*, 1082–1089. [[CrossRef](#)]
18. Kim, F.; Pham, M.; Maloney, E.; Rizzo, N.O.; Morton, G.J.; Wisse, B.E.; Kirk, E.A.; Chait, A.; Schwartz, M.W. Vascular Inflammation, Insulin Resistance, and Reduced Nitric Oxide Production Precede the Onset of Peripheral Insulin Resistance. *Arterioscler. Thromb. Vasc. Biol.* **2008**, *28*, 1982–1988. [[CrossRef](#)]
19. Kina-Tanada, M.; Sakanashi, M.; Tanimoto, A.; Kaname, T.; Matsuzaki, T.; Noguchi, K.; Uchida, T.; Nakasone, J.; Kozuka, C.; Ishida, M.; et al. Long-term dietary nitrite and nitrate deficiency causes the metabolic syndrome, endothelial dysfunction and cardiovascular death in mice. *Diabetologia* **2017**, *60*, 1138–1151. [[CrossRef](#)] [[PubMed](#)]
20. Matthys, K.E.; Bult, H. Nitric oxide function in atherosclerosis. *Mediators Inflamm.* **1997**, *6*, 3. [[CrossRef](#)]
21. Carlström, M.; Larsen, F.J.; Nyström, T.; Hezel, M.; Borniquel, S.; Weitzberg, E.; Lundberg, J.O. Dietary inorganic nitrate reverses features of metabolic syndrome in endothelial nitric oxide synthase-deficient mice. *Proc. Natl. Acad. Sci. USA* **2010**, *107*, 17716–17720. [[CrossRef](#)] [[PubMed](#)]
22. Shankar, R.R.; Wu, Y.; Shen, H.Q.; Zhu, J.S.; Baron, A.D. Mice with gene disruption of both endothelial and neuronal nitric oxide synthase exhibit insulin resistance. *Diabetes* **2000**, *49*, 684–687. [[CrossRef](#)] [[PubMed](#)]
23. Tsutsui, M.; Tanimoto, A.; Tamura, M.; Mukae, H.; Yanagihara, N.; Shimokawa, H.; Otsuji, Y. Significance of nitric oxide synthases: Lessons from triple nitric oxide synthases null mice. *J. Pharmacol. Sci.* **2015**, *127*, 42–52. [[CrossRef](#)]

24. Mao, K.; Chen, S.; Chen, M.; Ma, Y.; Wang, Y.; Huang, B.; He, Z.; Zeng, Y.; Hu, Y.; Sun, S.; et al. Nitric oxide suppresses NLRP3 inflammasome activation and protects against LPS-induced septic shock. *Cell Res.* **2013**, *23*, 201–212. [[CrossRef](#)] [[PubMed](#)]
25. Perreault, M.; Marette, A. Targeted disruption of inducible nitric oxide synthase protects against obesity-linked insulin resistance in muscle. *Nat. Med.* **2001**, *7*, 1138–1143. [[CrossRef](#)]
26. Spruss, A.; Kanuri, G.; Uebel, K.; Bischoff, S.C.; Bergheim, I. Role of the Inducible Nitric Oxide Synthase in the Onset of Fructose-Induced Steatosis in Mice. *Antioxid. Redox Signal.* **2011**, *14*, 2121–2135. [[CrossRef](#)] [[PubMed](#)]
27. Charbonneau, A.; Marette, A. Inducible Nitric Oxide Synthase Induction Underlies Lipid-Induced Hepatic Insulin Resistance in Mice: Potential Role of Tyrosine Nitration of Insulin Signaling Proteins. *Diabetes* **2010**, *59*, 861. [[CrossRef](#)]
28. Jang, J.E.; Ko, M.S.; Yun, J.-Y.; Kim, M.-O.; Kim, J.H.; Park, H.S.; Kim, A.-R.; Kim, H.-J.; Kim, B.J.; Ahn, Y.E.; et al. Nitric Oxide Produced by Macrophages Inhibits Adipocyte Differentiation and Promotes Profibrogenic Responses in Preadipocytes to Induce Adipose Tissue Fibrosis. *Diabetes* **2016**, *65*, 2516–2528. [[CrossRef](#)]
29. Dallaire, P.; Bellmann, K.; Laplante, M.; Gélinas, S.; Centeno-Baez, C.; Penfornis, P.; Peyot, M.-L.; Latour, M.G.; Lamontagne, J.; Trujillo, M.E.; et al. Obese mice lacking inducible nitric oxide synthase are sensitized to the metabolic actions of peroxisome proliferator-activated receptor-gamma agonism. *Diabetes* **2008**, *57*, 1999–2011. [[CrossRef](#)] [[PubMed](#)]
30. Cha, H.-N.; Song, S.E.; Kim, Y.-W.; Kim, J.-Y.; Won, K.-C.; Park, S.-Y. Lack of inducible nitric oxide synthase prevents lipid-induced skeletal muscle insulin resistance without attenuating cytokine level. *J. Pharmacol. Sci.* **2011**, *117*, 77–86. [[CrossRef](#)]
31. Nakata, S.; Tsutsui, M.; Shimokawa, H.; Suda, O.; Morishita, T.; Shibata, K.; Yatera, Y.; Sabanai, K.; Tanimoto, A.; Nagasaki, M.; et al. Spontaneous myocardial infarction in mice lacking all nitric oxide synthase isoforms. *Circulation* **2008**, *117*, 2211–2223. [[CrossRef](#)] [[PubMed](#)]
32. Kanuri, B.N.; Kanshana, J.S.; Rebello, S.C.; Pathak, P.; Gupta, A.P.; Gayen, J.R.; Jagavelu, K.; Dikshit, M. Altered glucose and lipid homeostasis in liver and adipose tissue pre-dispose inducible NOS knockout mice to insulin resistance. *Sci. Rep.* **2017**, *7*, 41009. [[CrossRef](#)] [[PubMed](#)]
33. Kakimoto, P.A.; Chausse, B.; Caldeira da Silva, C.C.; Donato Júnior, J.; Kowaltowski, A.J. Resilient hepatic mitochondrial function and lack of iNOS dependence in diet-induced insulin resistance. *PLoS ONE* **2019**, *14*, e0211733. [[CrossRef](#)]
34. Fujimoto, M.; Shimizu, N.; Kunii, K.; Martyn, J.A.J.; Ueki, K.; Kaneki, M. A Role for iNOS in Fasting Hyperglycemia and Impaired Insulin Signaling in the Liver of Obese Diabetic Mice. *Diabetes* **2005**, *54*, 1340–1348. [[CrossRef](#)] [[PubMed](#)]
35. Khedara, A.; Kawai, Y.; Kayashita, J.; Kato, N. Feeding Rats the Nitric Oxide Synthase Inhibitor, L-N ω -Nitroarginine, Elevates Serum Triglyceride and Cholesterol and Lowers Hepatic Fatty Acid Oxidation. *J. Nutr.* **1996**, *126*, 2563–2567. [[CrossRef](#)]
36. Goto, T.; Ohnami, S.; Khedara, A.; Kato, N.; Ogawa, H.; Yanagita, T. Feeding the nitric oxide synthase inhibitor L-N(omega)nitroarginine elevates serum very low density lipoprotein and hepatic triglyceride synthesis in rats. *J. Nutr. Biochem.* **1999**, *10*, 274–278. [[CrossRef](#)]
37. Aggarwal, H.; Kanuri, B.N.; Dikshit, M. Role of iNOS in Insulin Resistance and Endothelial Dysfunction. In *Oxidative Stress in Heart Diseases*; Springer: Singapore, 2019; pp. 461–482.
38. Milsom, A.B.; Fernandez, B.O.; Garcia-Saura, M.F.; Rodriguez, J.; Feelisch, M. Contributions of Nitric Oxide Synthases, Dietary Nitrite/Nitrate, and Other Sources to the Formation of NO Signaling Products. *Antioxid. Redox Signal.* **2012**, *17*, 422–432. [[CrossRef](#)]
39. Cha, H.-N.; Kim, Y.-W.; Kim, J.-Y.; Kim, Y.-D.; Song, I.H.; Min, K.-N.; Park, S.-Y. Lack of inducible nitric oxide synthase does not prevent aging-associated insulin resistance. *Exp. Gerontol.* **2010**, *45*, 711–718. [[CrossRef](#)]
40. Ghasemi, A.; Jeddi, S. Anti-obesity and anti-diabetic effects of nitrate and nitrite. *Nitric Oxide* **2017**, *70*, 9–24. [[CrossRef](#)]
41. Kleemann, R.; van Erk, M.; Verschuren, L.; van den Hoek, A.M.; Koek, M.; Wielinga, P.Y.; Jie, A.; Pellis, L.; Bobeldijk-Pastorova, I.; Kelder, T.; et al. Time-Resolved and Tissue-Specific Systems Analysis of the Pathogenesis of Insulin Resistance. *PLoS ONE* **2010**, *5*, e8817. [[CrossRef](#)]
42. Jiang, H.; Torregrossa, A.C.; Potts, A.; Pierini, D.; Aranke, M.; Garg, H.K.; Bryan, N.S. Dietary nitrite improves insulin signaling through GLUT4 translocation. *Free Radic. Biol. Med.* **2014**, *67*, 51–57. [[CrossRef](#)] [[PubMed](#)]

43. Ohtake, K.; Nakano, G.; Ehara, N.; Sonoda, K.; Ito, J.; Uchida, H.; Kobayashi, J. Dietary nitrite supplementation improves insulin resistance in type 2 diabetic KKAY mice. *Nitric Oxide* **2015**, *44*, 31–38. [[CrossRef](#)] [[PubMed](#)]
44. Ables, G.P.; Perrone, C.E.; Orentreich, D.; Orentreich, N. Methionine-Restricted C57BL/6J Mice Are Resistant to Diet-Induced Obesity and Insulin Resistance but Have Low Bone Density. *PLoS ONE* **2012**, *7*, e51357. [[CrossRef](#)]
45. Kanuri, B.N.; Rebello, S.C.; Pathak, P.; Agarwal, H.; Kanshana, J.S.; Awasthi, D.; Gupta, A.P.; Gayen, J.R.; Jagavelu, K.; Dikshit, M. Glucose and lipid metabolism alterations in liver and adipose tissue pre-dispose p47^{phox} knockout mice to systemic insulin resistance. *Free Radic. Res.* **2018**, *52*, 568–582. [[CrossRef](#)] [[PubMed](#)]
46. Sadaf, S.; Singh, A.K.; Awasthi, D.; Nagarkoti, S.; Agrahari, A.K.; Srivastava, R.N.; Jagavelu, K.; Kumar, S.; Barthwal, M.K.; Dikshit, M. Augmentation of iNOS expression in myeloid progenitor cells expedites neutrophil differentiation. *J. Leukoc. Biol.* **2019**, *106*, 397–412. [[CrossRef](#)]
47. Kanshana, J.S.; Rebello, S.C.; Pathak, P.; Kanuri, B.N.; Aggarwal, H.; Srivastava, V.; Khanna, V.; Singh, V.; Jagavelu, K.; Barthwal, M.K.; et al. Standardized fraction of *Xylocarpus moluccensis* fruits improve vascular relaxation and plaque stability in dyslipidemic models of atherosclerosis. *J. Ethnopharmacol.* **2018**, *213*, 81–91. [[CrossRef](#)] [[PubMed](#)]
48. Brial, F.; Le Lay, A.; Hedjazi, L.; Tsang, T.; Fearnside, J.F.; Otto, G.W.; Alzaid, F.; Wilder, S.P.; Venteclef, N.; Cazier, J.-B.; et al. Systems Genetics of Hepatic Metabolome Reveals Octopamine as a Target for Non-Alcoholic Fatty Liver Disease Treatment. *Sci. Rep.* **2019**, *9*, 3656. [[CrossRef](#)]
49. Becares, N.; Gage, M.C.; Voisin, M.; Shrestha, E.; Martin-Gutierrez, L.; Liang, N.; Louie, R.; Pourcet, B.; Pello, O.M.; Luong, T.V.; et al. Impaired LXR α Phosphorylation Attenuates Progression of Fatty Liver Disease. *Cell Rep.* **2019**, *26*, 984–995. [[CrossRef](#)]
50. Nozaki, Y.; Fujita, K.; Wada, K.; Yoneda, M.; Kessoku, T.; Shinohara, Y.; Imajo, K.; Ogawa, Y.; Nakamuta, M.; Saito, S.; et al. Deficiency of iNOS-derived NO accelerates lipid accumulation-independent liver fibrosis in non-alcoholic steatohepatitis mouse model. *BMC Gastroenterol.* **2015**, *15*, 42. [[CrossRef](#)]
51. Kubant, R.; Poon, A.N.; Sánchez-Hernández, D.; Domenichiello, A.F.; Huot, P.S.P.; Pannia, E.; Cho, C.E.; Hunschede, S.; Bazinet, R.P.; Anderson, G.H. A comparison of effects of lard and hydrogenated vegetable shortening on the development of high-fat diet-induced obesity in rats. *Nutr. Diabetes* **2015**, *5*, e188. [[CrossRef](#)]
52. Khedara, A.; Goto, T.; Morishima, M.; Kayashita, J.; Kato, N. Elevated Body Fat in Rats by the Dietary Nitric Oxide Synthase Inhibitor, L-N^ω Nitroarginine. *Biosci. Biotechnol. Biochem.* **1999**, *63*, 698–702. [[CrossRef](#)] [[PubMed](#)]
53. Sadowska, J.; Gębczyński, A.K.; Konarzewski, M. Metabolic risk factors in mice divergently selected for BMR fed high fat and high carb diets. *PLoS ONE* **2017**, *12*, e0172892. [[CrossRef](#)]
54. Gupta, A.; Beg, M.; Kumar, D.; Shankar, K.; Varshney, S.; Rajan, S.; Srivastava, A.; Singh, K.; Sonkar, S.; Mahdi, A.A.; et al. Chronic hyper-leptinemia induces insulin signaling disruption in adipocytes: Implications of NOS2. *Free Radic. Biol. Med.* **2017**, *112*, 93–108. [[CrossRef](#)] [[PubMed](#)]
55. Lu, M.; Li, P.; Pferdekamper, J.; Fan, W.; Saber, M.; Schenk, S.; Olefsky, J.M. Inducible nitric oxide synthase deficiency in myeloid cells does not prevent diet-induced insulin resistance. *Mol. Endocrinol.* **2010**, *24*, 1413–1422. [[CrossRef](#)] [[PubMed](#)]
56. Tenopoulou, M.; Doulias, P.-T.; Nakamoto, K.; Berrios, K.; Zura, G.; Li, C.; Faust, M.; Yakovishina, V.; Evans, P.; Tan, L.; et al. Oral nitrite restores age-dependent phenotypes in eNOS-null mice. *JCI Insight* **2018**, *3*. [[CrossRef](#)] [[PubMed](#)]
57. Gheibi, S.; Jeddi, S.; Carlström, M.; Gholami, H.; Ghasemi, A. Effects of long-term nitrate supplementation on carbohydrate metabolism, lipid profiles, oxidative stress, and inflammation in male obese type 2 diabetic rats. *Nitric Oxide* **2018**, *75*, 27–41. [[CrossRef](#)]
58. Larsen, F.J.; Schiffer, T.A.; Ekblom, B.; Mattsson, M.P.; Checa, A.; Wheelock, C.E.; Nyström, T.; Lundberg, J.O.; Weitzberg, E. Dietary nitrate reduces resting metabolic rate: A randomized, crossover study in humans. *Am. J. Clin. Nutr.* **2014**, *99*, 843–850. [[CrossRef](#)]
59. Hezel, M.P.; Liu, M.; Schiffer, T.A.; Larsen, F.J.; Checa, A.; Wheelock, C.E.; Carlström, M.; Lundberg, J.O.; Weitzberg, E. Effects of long-term dietary nitrate supplementation in mice. *Redox Biol.* **2015**, *5*, 234–242. [[CrossRef](#)] [[PubMed](#)]
60. Konrad, D.; Wueest, S. The Gut-Adipose-Liver Axis in the Metabolic Syndrome. *Physiology* **2014**, *29*, 304–313. [[CrossRef](#)] [[PubMed](#)]

61. Penforis, P.; Marette, A. Inducible nitric oxide synthase modulates lipolysis in adipocytes. *J. Lipid Res.* **2005**, *46*, 135–142. [[CrossRef](#)] [[PubMed](#)]
62. Puigserver, P.; Rhee, J.; Donovan, J.; Walkey, C.J.; Yoon, J.C.; Oriente, F.; Kitamura, Y.; Altomonte, J.; Dong, H.; Accili, D.; et al. Insulin-regulated hepatic gluconeogenesis through FOXO1–PGC-1 α interaction. *Nature* **2003**, *423*, 550–555. [[CrossRef](#)] [[PubMed](#)]
63. Perry, R.J.; Camporez, J.-P.G.; Kursawe, R.; Titchenell, P.M.; Zhang, D.; Perry, C.J.; Jurczak, M.J.; Abudukadier, A.; Han, M.S.; Zhang, X.-M.; et al. Hepatic acetyl CoA links adipose tissue inflammation to hepatic insulin resistance and type 2 diabetes. *Cell* **2015**, *160*, 745–758. [[CrossRef](#)] [[PubMed](#)]



© 2020 by the authors. Licensee MDPI, Basel, Switzerland. This article is an open access article distributed under the terms and conditions of the Creative Commons Attribution (CC BY) license (<http://creativecommons.org/licenses/by/4.0/>).